European Journal of Medicinal Chemistry 213 (2021) 113186

Contents lists available at ScienceDirect

European Journal of Medicinal Chemistry

journal homepage: http://www.elsevier.com/locate/ejmech

Research paper

In silico drug repositioning on F508del-CFTR: A proof-of-concept study on the AIFA library

Alessandro Orro [a, 1], Matteo Uggeri [a, b, 1], Marco Rusnati [c], Chiara Urbinati [c], Nicoletta Pedemonte [d], Emanuela Pesce [d], Marco Moscatelli [a], Rita Padoan [e], Elena Cichero [b], Paola Fossa [b], Pasqualina D'Ursi [a, *]

[a] Institute for Biomedical Technologies, National Research Council (ITB-CNR), Segrate, MI, Italy
[b] Department of Pharmacy, Section of Medicinal Chemistry, School of Medical and Pharmaceutical Sciences, University of Genova, Genova, Italy
[c] Department of Molecular and Translational Medicine, University of Brescia, Brescia, Italy
[d] UOC Genetica Medica, IRCCS Istituto Giannina Gaslini, Genova, Italy
[e] Department of Pediatrics, Regional Support Centre for Cystic Fibrosis, Children's Hospital–ASST Spedali Civili, University of Brescia, Brescia, Italy

ARTICLE INFO

Article history:
Received 26 June 2020
Received in revised form
7 January 2021
Accepted 7 January 2021
Available online 13 January 2021

Keywords:
Cystic fibrosis
Drug repositioning
Molecular docking
Molecular dynamics
Surface plasmon resonance

ABSTRACT

Computational drug repositioning is of growing interest to academia and industry, for its ability to rapidly screen a huge number of candidates in silico (exploiting comprehensive drug datasets) together with reduced development cost and time.

The potential of drug repositioning has not been fully evaluated yet for cystic fibrosis (CF), a disease mainly caused by deletion of Phe 508 (F508del) of the cystic fibrosis transmembrane conductance regulator (CFTR) protein. F508del-CFTR is thus withheld in the endoplasmic reticulum and rapidly degraded by the ubiquitin/proteasome system.

CF is still a fatal disease. Nowadays, it is treatable by some CFTR-rescuing drugs, but new-generation drugs with stronger therapeutic benefits and fewer side effects are still awaited.

In this manuscript we report about the results of a pilot computational drug repositioning screening in search of F508del-CFTR-targeted drugs performed on AIFA library by means of a dedicated computational pipeline and surface plasmon resonance binding assay to experimentally validate the computational findings.

1. Introduction

"Drug repositioning", also termed "drug repurposing" is by now a validated alternative strategy to accelerate the drug development process by seeking new indications for already approved drugs, rather than discovering de novo active compounds [1]. Its success development strategy for the pharmaceutical industry is due to its capacity of strongly decreasing the average cost and time of developing a drug, as several development steps can be minimized, while avoiding the occurrence of unforeseen adverse events. Thus, from the initial repositioning of thalidomide and its approval for multiple myeloma in 2012, many other drugs were successfully repositioned, minoxidil, imatinib, sildenafil, methotrexate, and propranolol, for citing some among the many already historical examples.

The increasing appeal of the repositioning technique also for government and academic institutions, as documented by the amount of scientific literature concerning this topic, is undoubtedly determined by its elective applicability in finding drugs for the treatment of orphan, rare or new disorders (see as an example its wide application in the 2020 COVID-19 pandemic). In this task, drug repositioning is strongly supported by bioinformatics, which makes available potent and advanced computational tools for the screening of large databases in a short time [2,3].

Cystic fibrosis (CF) is the most common monogenic disorder in Caucasians. It is characterized by the over-production of a thick mucus causing the impairment of innate defence against bacteria [4] with consequent recurrent pulmonary infections. Eventually, this will result in progressive loss of respiratory function [5,6].

* Corresponding author. Institute for Biomedical Technologies, National Research Council (ITB-CNR), Via Fratelli Cervi 93, 20090 Segrate, MI, Italy.
E-mail address: pasqualina.dursi@itb.cnr.it (P. D'Ursi).
[1] the Authors contributed equally to the work.

https://doi.org/10.1016/j.ejmech.2021.113186
0223-5234/

CF is due to various mutations in the cystic fibrosis transmembrane conductance regulator (CFTR) [7]. The most common mutation is the deletion of the triplet CTT involving codons 507 and 508 of the CFTR gene, that eliminates a phenylalanine (F508del). In turn, it causes inappropriate folding and instability of the F508del-CFTR protein that remains thus trapped in the endoplasmic reticulum with its rapid degradation by the ubiquitin/proteasome system [8].

Current therapies are mostly aimed at the clinical management of bacterial lung infections and consequent inflammation trying to prevent the progressive loss of respiratory function. Although these therapies have significantly pushed forward the mean survival age of patients [9], the burden of CF care remains very high and life quality and expectancy for most CF patients are still limited. This calls for therapeutic alternatives addressing CF systemically, by means of small molecules able to rescue the function of the mutated CFTR.

This approach has already led to the development of four compounds that are currently on the market: lumacaftor (VX809), ivacaftor (VX770), tezacaftor (VX661), elexacaftor (VX445) and their combinations [10], among which the recently approved Trikafta [11,12].

These new therapies resulted in significant benefits for CF patients as described both in Randomized Controlled Trials (RCTs) and studies on data from national CF registries [13,14], but also some adverse events mainly consisting in cough, nasopharyngitis, oropharyngeal pain, and upper respiratory tract infection [15]. In addition, depression, anxiety, sleep paralysis with hypnopompic hallucinations [16] and testicular pain [17] have been reported after initiation of Trikafta therapy. Another common adverse event reported in patients treated with CFTR modulators is an abnormal liver function that is however moderate in severity and did not require drug discontinuation [18].

A further issue calling for more efforts in the development of new treatment is the high cost of CFTR modulators currently approved. In particular, CF therapies and care in low and middle-income countries (LMIC) need to be adapted to available resources of these countries where the cost of CFTR modulators appears to be prohibitive [19].

Thus, despite the evident progress in the field of CF drug discovery, new, possibly more efficacious and less expensive CF drugs devoid of adverse effects are eagerly awaited.

As already mentioned above, drug repurposing is a technique already successfully employed to reposition some drugs for the treatment of various diseases. Concerning CF, drug repurposing has been taken in consideration only for pulmonary delivery of inhaled antibiotics [20] and to enhance mucociliary clearance [21], but its exploitation to circumvent CFTR dysfunction has been to date only suggested [22,23].

2. Results

2.1. Computational drug repositioning

AIFA database includes 1130 compounds from which inorganic salts, peptides, proteins, and hormones were removed, leaving 846 small-molecule drugs already approved for the therapy of other diseases and nutraceuticals.

The drugs of the data set were evaluated for their capability to bind F508del-CFTR by means of a suitable F508del-CFTR 3D model available to date (further described below) and an *ad hoc* designed pipeline, whose first part (Fig. 1, part A) overlaps that already used in our previous work to identify the druggable pocket 1 (DP1) by using VX809 as template [24].

Here, DP1 has been used in our pipeline (Fig. 1, part B) to screen the 846 compounds of the AIFA database. Docking repositioning results (Supplementary Table 1) were firstly filtered by energy, taking in consideration only those poses with docking energies like that of VX809.

Then a visual inspection (H-bonds) of the 3D poses interaction pattern and, again, a comparison with the VX809 binding mode [24] allowed the selection of 11 drugs repositioned on F508del-CFTR (Fig. 2).

The 11 repositioned drugs show different chemical scaffolds and include a natural compound, rutin, the glycoside of the flavonol quercetin, and synthetic drugs such as imatinib, nilotinib, doxorubicin, bexarotene, aprepitant, eltrombopag, gliquidone, tadalafil, telmisartan and zafirlukast.

From our previous findings [24], VX809 localizes at the NBD1-NBD2 interface, partially flanking ICL4. H-bond interactions occur with S492, S495, W496 of NBD1, W1063 of ICL4 and C1344 of NBD2. Lipophilic interactions occur instead with D173 of ICL1, W401, F490, F494 and W496 of NBD1, T1064 of ICL4 and V1345 of NBD2. Finally, a $\pi-\pi$ staking occurs with W1063 of ICL4 and a salt bridge with R560 of NBD1 (Table 1).

Imatinib, rutin, doxorubicin, tadalafil, telmisartan, zafirlukast and gliquidone show a common H-bonding pattern with VX809 (one or more interaction with S492, W496, W1063). Also, all the repositioned drugs show two or more lipophilic interactions involving common residues with VX809. $\pi-\pi$ stacking with W1063 has been observed only for imatinib, nilotinib, eltrombopag, tadalafil, telmisartan, aprepitant and gliquidone. Imatinib, nilotinib, eltrombopag, tadalafil, telmisartan, aprepitant, zafirlukast and bexarotene show also a π-cation interaction involving K1351. None of them is able to display the salt bridge with R560 shown by VX809.

The comparison of the binding modes of the repositioned drugs with VX809 indicated that, even if sharing the above reported common interactions with the template, they display different ability in occupying the large DP1, and interact with the surrounding amino acidic residues from NBD1, NBD2 and ICL4. Accordingly, the selected drugs are almost unable to fully overlap VX809, except for telmisartan, zafirlukast and tadalafil. Most of them instead limit their overlapping on VX809 to that area defined by the aromatic ring bringing the carboxylic group and the adjacent carbons of the pyridinic ring. In addition, lipophilic interactions seem to play a predominant role over polar interactions in anchoring the drugs to residues in NBD1, NBD2 and ICL4.

In order to better ascertain the probability of these residues to be located into the best druggable pocket along the Molecular Dynamics (MDs), Fpocket software has been applied [25] on the F508del CFTR apo form MDs to monitor the residues located in a range of 4 Å in the VX809 complex. As shown in supplementary material Fig. S1, Fpocket often assigns to these amino acids a very high probability to be part of a druggable pocket (druggability score = 70–80%). This probability has a periodic shape, proving that these residues during the MDs periodically can interact with a ligand in an efficient manner.

In conclusion, contextualizing the docking results inside DP1, three typologies of drugs can be defined depending on the location of residues involved in the binding:

(1) the most populated group corresponding to those drugs able to bridge NBD1 and NBD2, binding also to residues of the ICL4 domain. These are VX809 itself, doxorubicin, nilotinib, aprepitant, bexarotene, eltrombopag, zafirlukast and rutin.
(2) drugs that mostly occupy DP1 taking close interactions with residues in NBD1 and ICL4. These correspond to imatinib, tadalafil and telmisartan.

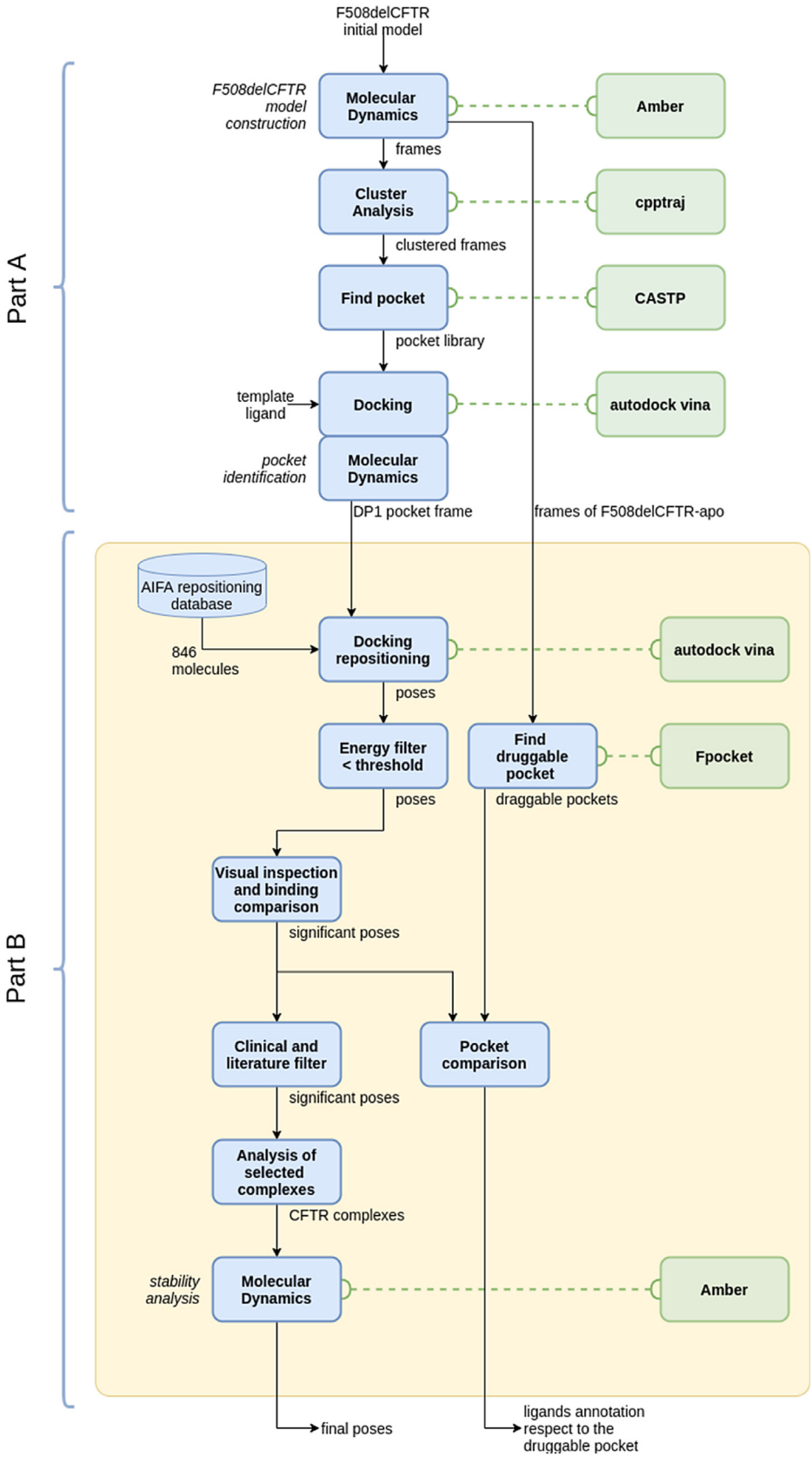

Fig. 1. Schematic representation of the computational drug repositioning pipeline. Part A of the pipeline has been previously described in detail in Ref. [24]. Part B, starts from a selected pocket (DP1) to perform the docking simulations against the AIFA drug database.

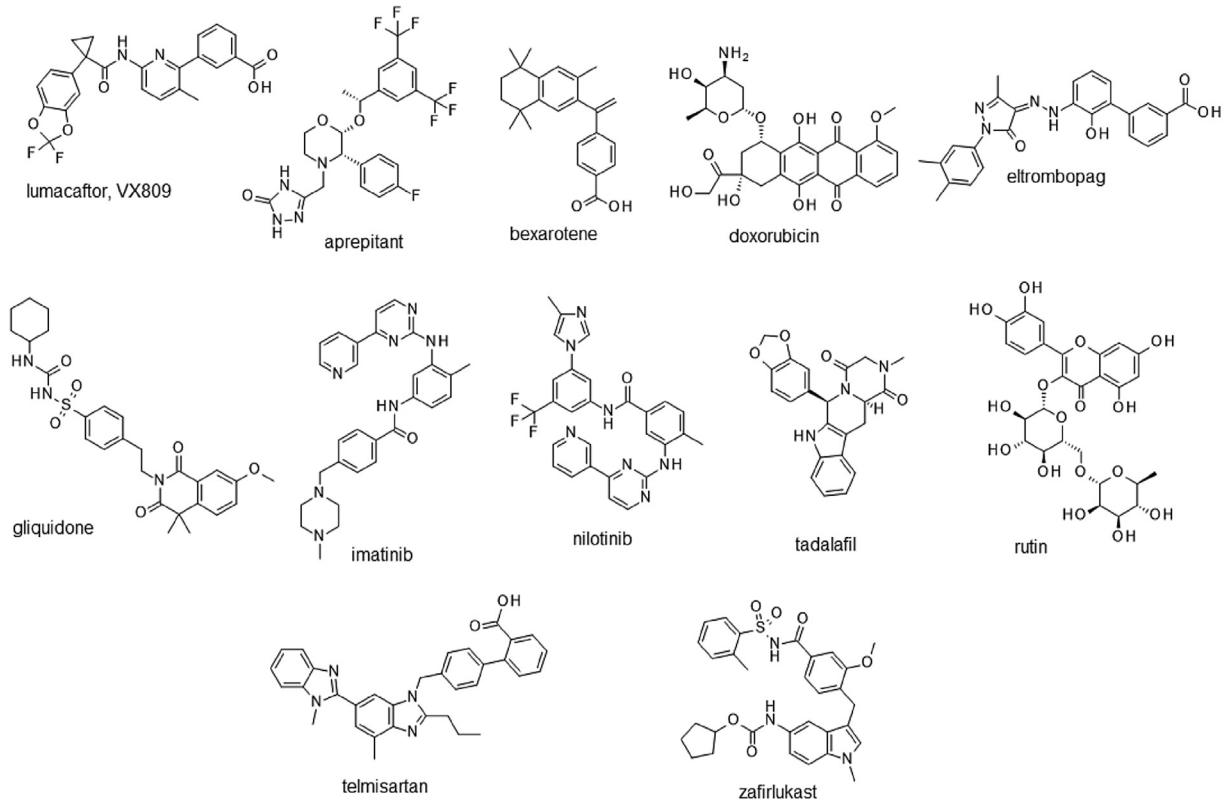

Fig. 2. Chemical structures of the repositioned drugs. In figure are reported the 2D structure of the 11 drugs repositioned: VX809 (template), aprepitant, bexarotene, doxorubicin, eltrombopag, gliquidone, imatinib, nilotinib, rutin tadalafil, telmisartan and zafirlukast.

(3) gliquidone is the only member of the third group, displaying interactions only with the apical region of NBD1.

Interestingly, superimposing one ligand for each group to VX809, it is possible to appreciate three different space sub-regions around the aromatic acid portion of the template, which are not occupied by VX809 itself but could be possibly occupied by other drugs, thus deserving further investigation (Fig. 3).

Fpocket analysis has been thus performed in the same way as described above, on rutin, imatinib, gliquidone (representatives for the three groups). The corresponding plots are reported as supplementary material (Fig. S2, S3 and S4, respectively). From these plots is evident that in the apo form of F508del CFTR, residues surrounding imatinib appear endowed of a high probability/druggability score (70–80%) along all the MDs, comparable to that of VX809.

Residues located around rutin and gliquidone show a high average score only in the latest part of the MDs. For all compounds, the plot has a periodic shape, indirectly suggesting that F508del CFTR periodically exposes selected residues for the interaction with a ligand. We can infer that in the case of imatinib and VX809, the binding pocket residues have a high possibility to be available for the interaction.

2.2. Clinical assessment and selection of the repositioned drugs

The 11 repositioned drug and food compounds have been subjected to a clinical evaluation on the basis of the AIFA and EMA documents [www.farmaci.agenziafarmaco.gov.it and www.ema.europa.eu].

The most populated group of repositioned drugs is represented by antineoplastic agents:

Doxorubicin causes cardiotoxicity, arrhythmias, congestive heart failure at the doses required to exert its antineoplastic effect. **Nilotinib and imatinib** cause prolongation of the QT tract. They can then interfere with other drugs used in CF, such as azole antifungals or macrolide antibiotics. **Bexarotene** is contraindicated in subjects with or at risk of pancreatitis. Relevantly, a frequency of recurrent/chronic pancreatitis between 17% and 22% is estimated in patients with CF [26]. Common side effects of antineoplastic drugs are also nausea, vomiting, diarrhea, alopecia and stomatitis and, overall, bone marrow depression with consequent increased risk of infections, that are extremely dangerous in CF patients already at risk of malnutrition and bacterial, viral and fungal respiratory infections.

Aprepitant is an antiemetic used in chemotherapy. It may cause neutropenia, thus increasing the risk of infections. **Zafirlukast** is a leukotriene receptor antagonist used to alleviate the symptoms of asthma by preventing bronchial smooth muscle contraction, edema of the airways, increased mucus secretion and eosinophils recruitment. Although a pilot study assessed its efficacy as anti-inflammatory agent in adult CF patients [27], possible side effects have been then reported consisting in breathing difficulties, jaundice, nausea, headache or excessive tiredness, as well as important psychological problems such as agitation, anxiety, irritability, aggression, hallucinations, depression, restlessness, tremors. In AIFA, Zafirlukast has been classified as a second-choice drug due to its not yet completely clarified side-effects, and from 2017 it has been withdrawn. **Eltrombopag** is indicated in patients (age>1 year) for the treatment of refractory chronic autoimmune thrombocytopenic purpura. Its severe hepatotoxicity and the risk of thrombotic or thromboembolic complications make it unsuitable for CF patients. **Gliquidone** is an oral hypoglycemic contraindicated in type I diabetes. For this reason, it does not seem appropriate for

Table 1
Binding energy ranking of the repositioned drugs. The residues are reported as one-letter code. The interaction pattern is listed. Apex numbers indicate the number of interactions displayed by different ligand atoms with the same amino acid residue, while * indicates interaction residues common with VX809.

Compound	H-bond interactions		Hydrophobic interactions		$\pi-\pi$ staking interactions		π -cation interactions		Binding energy
	docking	MDs	docking	MDs	docking	MDs	Docking	MDs	
Rutin	// // W496[3]* // // R560[2] // V1056 T1057[2] K1060 T1064 // D1341 G1342 K1351	E267 S492* W496* I497[2] G544 // D572 // T1057 // T1064[2] V1293 // // K1351	I266 F490* W496* T1064* //	// // W496* T1064* //	//	F494			−13.1
telmisartan	// W1063*	S169 W1063[2]*	L172[3] T465 // W496[2]* D572 L801 K1060 // T1064*	// // F494[2] W496* // // // W1063 //					−12.4
eltrombopag	Q1071 K1351		E201 F494[2] W496[2]* L804[2] K1060 V1293 F1294 K1351		F494 W496[2]		K1060 K1351		−12,3
zafirlukast	W1063* T1064 K1351		L172[2] D173* I177 W496* L804 K1060[2] W1063 F1068		F494		K1351		−12.1
nilotinib	E 201 K1060 Q1071 K1351		E201 W496[2]* T1064* F1068[2] V1293 F1294 K1351		W496		K1351		−12.0
doxorubicin	S492* R560 K1060 V1293 K1351		W496[2]* L804 W1063[2] T1064* F1068						−11.8
imatinib	S492* K1351		T465 L468 W496* D572 W1063 T1064*		W1063[2]*		K1351		−11.8
tadalafil	// // W1063* //	S492* K1060 // K1351	W496* L804 T1057 K1060 W1063 //	W496* // // // // T1064*	W496 W1063*	// //	//	K1351	−11.8
VX809 (template)	S492[2]* S495 W496* W1063* C1344		D173* W401 F490* F494[3]* W496*		W1063*				−11,6

(*continued on next page*)

Table 1 (*continued*)

Compound	H-bond interactions		Hydrophobic interactions		$\pi-\pi$ staking interactions		π -cation interactions		Binding energy
	docking	MDs	docking	MDs	docking	MDs	Docking	MDs	
			T1064* V1345						
gliquidone	S492* F494 K1060 K1351		T465 L468 F490* F494[2]* W496[2]* D572		F494 W496[2]				−11.5
aprepitant	K1060 T1064		F490* F494[2]* W496* W1063 T1064* F1068 V1293 K1351		F494		K1351		−11.3
bexarotene	K1351[2]		F494[5]* W496* T1064* V1293 F1294 K1351				K1351		−11.1

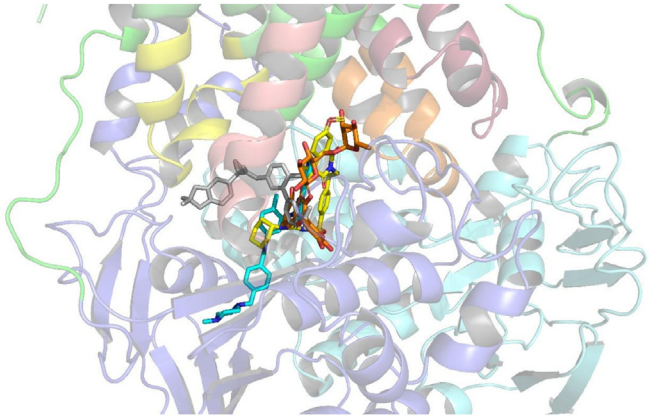

Fig. 3. Superimposition of imatinib, gliquidone and rutin on VX809. The four drugs are shown as colored sticks: VX809 in grey, gliquidone in yellow, rutin in orange, imatinib in cyan; while F508del-CFTR in cartoon: NBD1 in slate blue, NBD2 in cyan, ICL1 in yellow, ICL2 in orange, ICL3 in raspberry red, ICL4 in salmon pink, and TMs in green.

CF patients that, due to a decrease of insulin secretion, are at risk of developing diabetes in a significant percentage in adolescence and adulthood [28]. **Telmisartan** is an angiotensin II receptor antagonist (ARBs) used to treat essential hypertension in adults and to reduce cardiovascular morbidity in patients with type 2 diabetes mellitus [29]. As mentioned above, CF patients are at risk of developing diabetes, making telmisartan an interesting drug. However, it should not be administered to patients with biliary tract obstructions or liver failure as it is mainly eliminated with bile. Relevantly, liver disease is estimated to occur in around 10% of patients with CF [30]. **Tadalafil** is a phosphodiesterase 5 inhibitor. In an *in vivo* model of ischemia tissue damage, it decreases TNF-α, IL-1β, and IL-6 production with consequent anti-inflammatory effects. More importantly, anti-phosphodiesterase 5 drugs can activate the chloride channel in homozygous F508del mice [31]. **Rutin** (or rutinose) is a nutraceutical glycoside, composed by the flavonoid quercetin and rutinose, which is bio-converted in quercetin (further detailed below). Rutin/quercetin are endowed with a broad spectrum of biological effects among which reduction of venous insufficiency and capillary fragility plus an anti-inflammatory potential that seems to be the most interesting from the CF patient's point of view, as inflammation is the initial actor of lung damage already at an early age [32].

In conclusion, combining the information derived by the binding energy ranking of the repositioned drugs and their clinical assessment, we decided to focus on telmisartan, tadalafil and rutin for further computational ad experimental evaluation.

2.3. Complex stability and molecular interactions of the repositioned drugs

Tadafil, telmisartan and rutin have been then submitted to three independent MDs with different initial velocity to test the stability of their complexes with F508del-CFTR and to fix their binding pose into the protein [33–35]. A structural analysis of all replicas show that the initial binding mode of each ligands is kept (RMSD lower than 2 Å from the starting docking pose) except for a single rutin run.

Subsequently, for each ligand, for the poses with RMSD lower than 2 Å we performed binding free energy calculations and the pose with lowest energy was selected as the correct binding mode (Fig. S5). Related RMSD analysis of the complexes show a good stability of the whole system, with rutin, telmisartan and tadalafil reaching stability after 5 ns, 12 ns and 2 ns, respectively (Fig. S6).

RMSF comparison of the three complexes with the apo F508del-CFTR shows a general lower or equal fluctuation of complexes. In particular, tadalafil, telmisartan, and rutin (Figs. 4A, 5A and 6A, respectively) stabilize part of the NBD1 domain, while part of NBD2 is stabilized only by rutin and tadalafil.

Moreover, rutin is the only compound able to stabilize the ICL4 domain, while telmisartan produces a higher ICL4 fluctuation when compared to the apo form. Then, the comparison between rutin and VX809 RMSF analyses show how the two drugs have a comparable stabilizing capability over F508del-CFTR. Rutin efficiently stabilizes NBD1, ICL4 and NBD2, the main regions involved in CFTR rescue. In the case of VX809, a lower stabilizing effect of the drug over F508del-CFTR can be observed limited to the N-terminal part of ICL4 (Fig. 7).

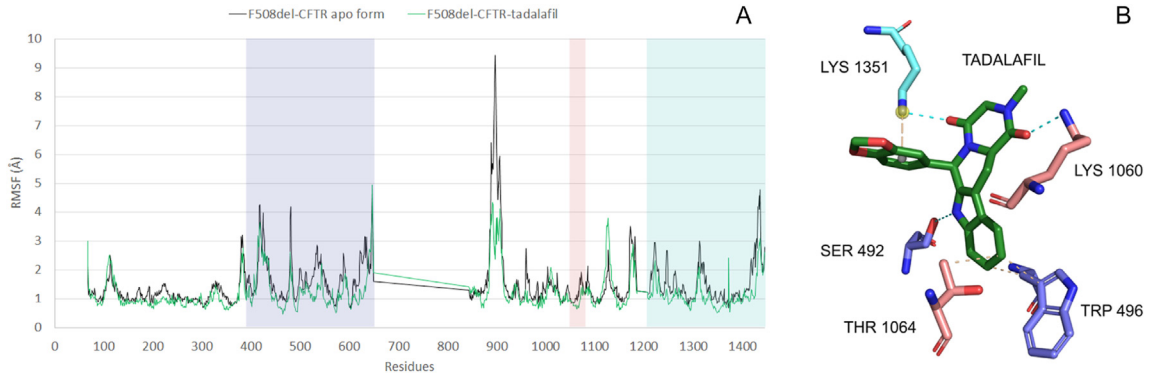

Fig. 4. RMSF and binding mode interactions for tadalafil complex. (*A*) *Cα comparison between F508del-CFTR apo form and complexed with tadalafil. F508del-CFTR apo form is colored in black and tadalafil in green. The colored boxes represented the NBD1, ICL4, and NBD2 colored as slate blue, salmon pink and cyan, respectively.* (*B*) *The binding mode of tadalafil with F508del-CFTR after MDs. H-bonds and hydrophobic interactions are colored as cyan and ochre dashed dots, respectively, while π-cation interactions are shown as yellow spheres. F508del-CFTR residues are shown as sticks and colored as follows: NBD1 slate blue, ICL4 salmon pink, NBD2 cyan.*

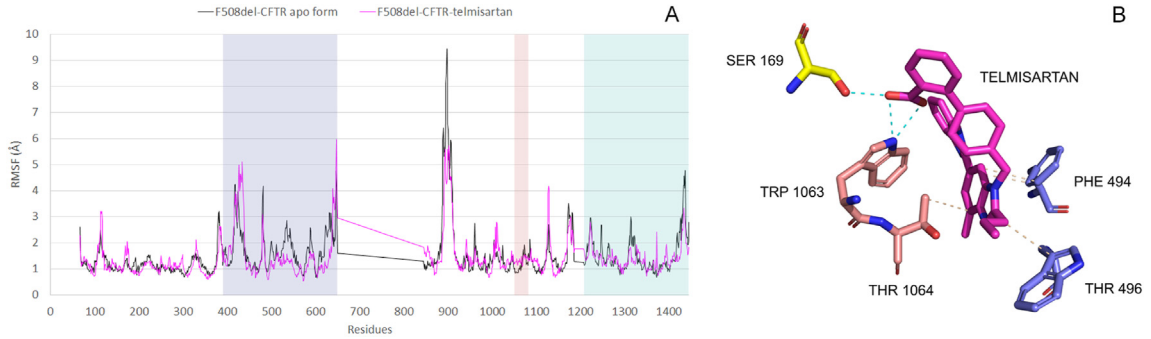

Fig. 5. RMSF and binding mode interactions for the telmisartan complex. (A) Cα comparison between F508del-CFTR apo form and complexed with telmisartan. F508del-CFTR apo form is colored in black and telmisartan in magenta. The colored boxes represented the NBD1, ICL4, and NBD2 colored as slate blue, salmon pink and cyan, respectively. (B) The binding mode of telmisartan with F508del-CFTR after MDs. H-bonds and hydrophobic interactions are colored as cyan and ochre dashed dots, respectively. F508del-CFTR residues are shown as sticks and colored as follows: ICL1 yellow, NBD1 slate blue, ICL4 salmon pink.

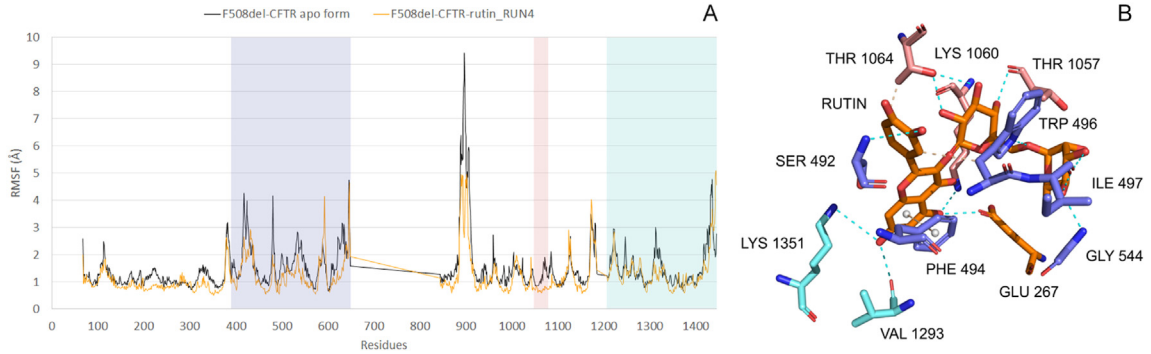

Fig. 6. RMSF and binding mode interactions for rutin complex. (A) Cα comparison between F508del-CFTR apo form and complexed with rutin. F508del-CFTR apo form is colored in black, rutin in orange. The colored boxes represented the NBD1, ICL4, and NBD2 colored as slate blue, salmon pink and cyan, respectively. (B) The binding mode of rutin with F508del-CFTR after MDs. H-bonds and hydrophobic interactions are colored as cyan and ochre dashed dots, respectively, while π-cation interactions are shown as white spheres. F508del-CFTR residues are shown as sticks and colored as follows: ICL1 orange, NBD1 slate blue, ICL4 salmon pink, and NBD2 in cyan.

Interactions after MDs for the studied compounds are detailed in Table 1.

Tadalafil slightly moves towards the NBD2 domain and increases the number of its H-bond with the protein. It loses the interaction with W1063 observed in the VX809 complex, but engages interactions with residues S492, K1060 and K1351 (Fig. 4B). The number of lipophilic interactions is decreased in comparison with the docking pose, however, the interaction with W496 is maintained and an interaction with T1064 is gained. Moreover, a π-cationic interaction is displayed with K1351. Related RMSD analyses are shown in Fig. S5.

Telmisartan increases its H-bonds interaction by involving S169 of ICL1, plus W1063 (shared with VX809) (Fig. 5B), and it durably gains these two interactions after ~12 ns. Lipophilic interactions decrease, with only those with W496 and T1064 maintained and reinforced by F494. At variance, the π-cation interaction with K1351 of NBD2 is lost.

Rutin increases the number of H-bonds, thanks to its sugar

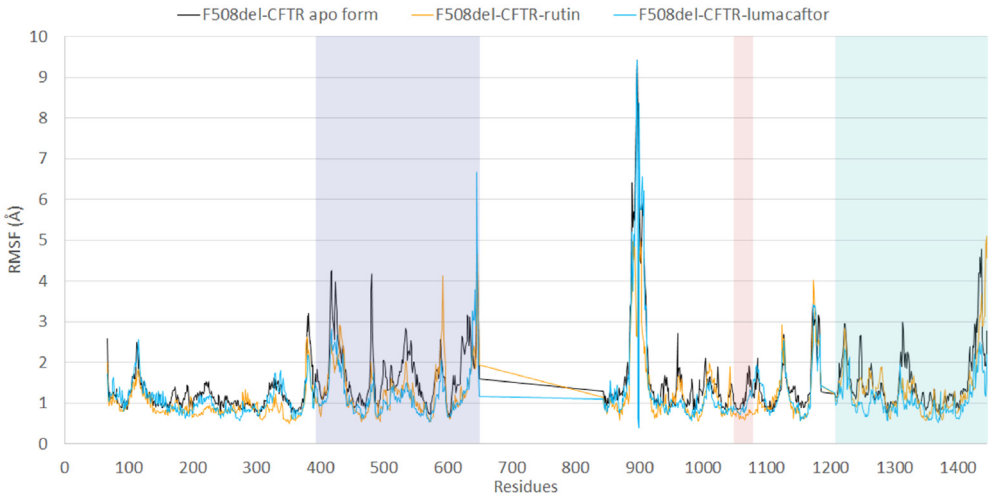

Fig. 7. RMSF comparison of rutin and VX809 complexes. Cα comparison between F508del-CFTR apo form and complexed with rutin and VX809. F508del-CFTR apo form is colored in black, rutin in orange and VX809 in cyan. The colored boxes represented the NBD1, ICL4, and NBD2 colored as slate blue, salmon pink and cyan, respectively.

moieties (Fig. 6B). It gains interactions with I497, G544 and D572, while keeping those with W496 (shared with VX809), T1057 and T1064. During MDs rutin slightly moves back to the NBD1 domain, thus losing the interaction with D1341 of NBD2. No additional lipophilic interactions were observed, while one π−π staking interaction is displayed with F494.

As written above, the three ligands partially superimpose to VX809 in the binding pocket, with tadalafil and telmisartan performing better than rutin, whose sugar moieties are directed to a region of DP1 not occupied by any of the other three molecules.

2.4. SPR analysis of the binding of the repositioned drugs to F508del-CFTR

A virtual interaction predicted in a computational drug repositioning protocol needs to be experimentally validated. SPR is a solid-phase optical-based technology that allows the evaluation of the actual interaction of target proteins with putative drugs. It represents an ideal technology to verify virtual interactions and obtain results that, in turn, are themselves predictive of the therapeutic potential of the analyzed drugs [36]. To this aim, tadalafil, telmisartan and rutin, predicted to act as F508del-CFTR binder, were evaluated for their effective capacity to bind to F508del-CFTR by exploiting the biosensor recently described by us in which the protein is immobilized in membrane-like lipid vesicles as to resemble the F508del-CFTR environment *in vivo* [24]. As shown in Fig. 8, the injection of increasing concentrations of the compounds tested onto the biosensor containing F508del-CFTR provided dose-dependent binding curves, with that from VX809 showing a steeper bending in respect to telmisartan and tadalafil, due to a significant binding of VX809 also at low concentrations. Accordingly, VX809 binds F508del-CFTR with an affinity that is significantly higher than those of telmisartan and tadalafil (Table 2). Interestingly, rutin shows an affinity that is only slightly lower than that of the reference compound (Table 2), emerging as the most promising F508del-CFTR-binder among the repositioned drugs identified.

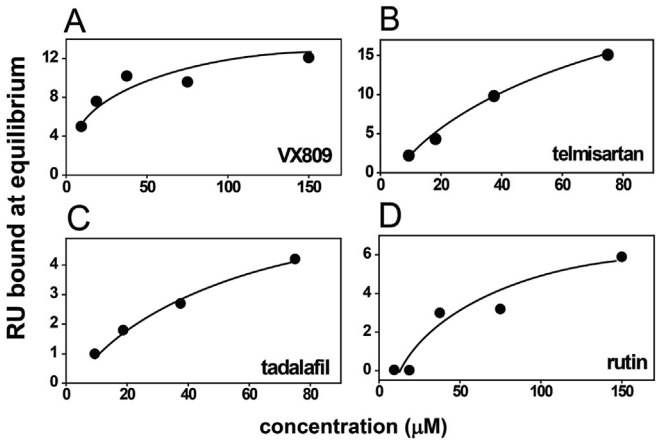

Fig. 8. Steady-state SPR analysis. The indicated compounds were injected onto the F508del-CFTR-containing biosensor at increasing concentrations. The results shown are representative of the other three experiments that gave similar results.

It must be pointed out however that rutin is promptly bioconverted in the flavonol quercetin (Fig. 9A) by human gut bacteria [37,38], making unlike an actual interaction between rutin and F508del-CFTR *in vivo* and calling for computational and experimental studies aimed at evaluating if quercetin retains F508del-CFTR-binding capacity. This also in light of the fact that quercetin has already been demonstrated to activate CFTR in gut [39] and airway epithelial cells [39,40].

2.5. Computational and biochemical validation of quercetin/F508del-CFTR interaction

To evaluate if quercetin (Fig. 9A) retains it CFTR-binding capacity docking simulations were performed (Fig. 9B). They confirmed that quercetin is able to fit in the DP1 almost occupying in the same region already involved in the binding by the aglyconic portion of

Table 2
Binding of the compounds to sensorchip-immobilized F508del-CFTR. Kd values are reported in μM ± S.E.M. The number of repeated independent calculations are indicated in brackets.

Compound	Kd (μM)
VX809 (template)	47.8 18.36 (5)
telmisartan	189.3 ± 48.5 (3)
tadalafil	175.0 ± 50.4 (4)
Rutin	65.8 ± 27.3 (7)
quercetin	25.6 ± 10.2 (3)

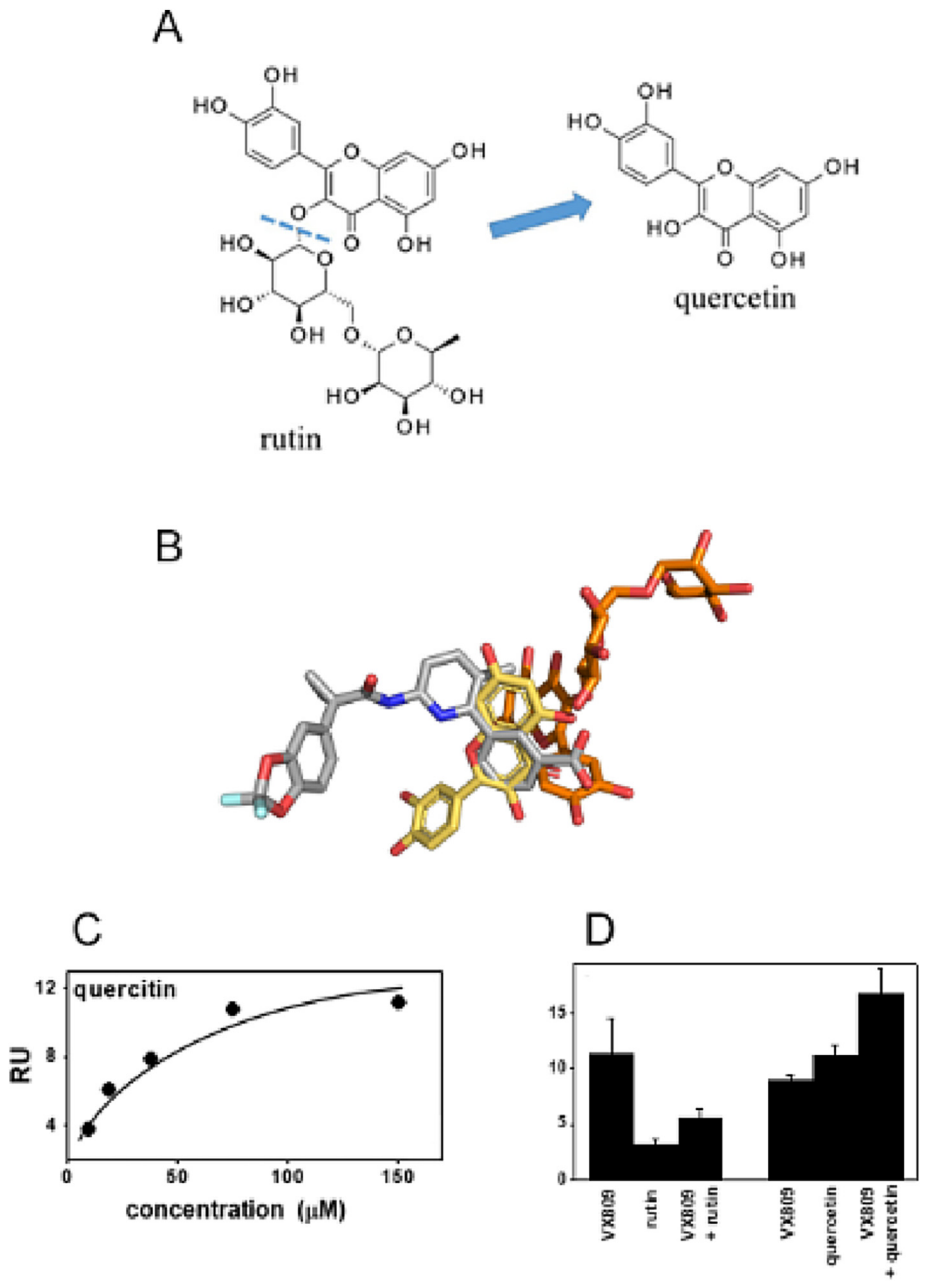

Fig. 9. Quercetin. (A) 2D chemical structure of rutin and its bioconversion to quercetin. (B) Superimposition of VX809 (grey), rutin (orange) and quercetin (yellow). (C) Steady-state SPR analysis of quercetin injected onto the F508del-CFTR-containing biosensor. The results shown are representative of the other three experiments that gave similar results. (D) SPR competition experiments: VX809 was injected onto the F508del-CFTR biosensor in the absence or in the presence of rutin or quercetin. The values of RU bound at equilibrium reported are the means ± S.E.M of 3–10 independent experiments.

rutin. In details, we observed a shift of about 180° of the isoflavonolic scaffold in comparison with rutin. The molecule appears to be superimposed with VX809 limited to the aromatic ring substituted with the carboxylic function.

Interestingly, SPR analysis demonstrated that quercetin binds F508del-CFTR in a dose-dependent and saturable manner (Fig. 9C) with an affinity that is comparable to that of VX809 itself (Table 2).

The fact that the repositioned drugs were selected on their predicted capacity to dock into the VX809 region in DP1 prompted us to perform competition binding assays between the VX809 and rutin or quercetin. As shown in Fig. 9D, at the doses tested, rutin partially inhibits VX809 binding to F508del-CFTR while quercetin shows instead an additive effect, suggesting that, due to its small dimension, it succeed in fitting in the DP1 of F508del-CFTR together with VX809.

3. Discussion

This work represents a "feasibility study" of a computational drug repositioning approach for the identification of new drugs to treat CF. In general, a computational drug repositioning program needs to start from an optimal computational model of the target protein. To this aim, here we have exploited the computational model of F508del-CFTR in a lipid environment that has been already used to study the binding modes of well-known and putative F508del-CFTR-rescuing drugs [24] providing predictions

with a high degree of consensus with experimental data [36], thus indicating its validity.

Another requisite for a successful computational repositioning program is the availability of appropriate drug databases. Due to the "proof-of-concept" nature of this work, we have so far focused our attention on the AIFA database, containing a relatively limited number of drugs. Nevertheless, we have been able to come up with 11 repositioned drugs, reduced to 3 after the clinical filter. This represents a promising result, in view of future similar computational drug repositioning programs on larger databases such as DrugBank and Dictionary of Natural Products.

Interestingly, among the repositioned compounds, tadalafil has been already taken in consideration for CF therapy [31].

The most populated group of repositioned drugs identified in this first attempt is that of antineoplastic agents, that have been excluded due to their severe side effects. However, since these side effects are manifested at doses high enough to exert the antineoplastic effect, it is likely that the same drugs may require lower (and thus safer) doses to exert their CFTR-rescuing activity, making them worth of further investigation as putative CF drugs. Accordingly, an *in vitro* study performed in 2007 demonstrated a positive effect on F508del-CFTR by doxorubicin [41], without however, no further evaluations on CF animal models or patients. Interesting is also the case of imatinib, that has been already repositioned in the past: developed and approved to target BCR-ABL in chronic myeloid leukaemia, some years later was repositioned, still in the oncological area, to target KIT in gastrointestinal stromal tumors [42].

Also worth of note is the observation that bexarotene, nilotinib and telmisartan have been selected in a drug repositioning program for Alzheimer disease [1] and, again, telmisartan in another repositioning program for *trans*-sialidase inhibitors of *Trypanosoma cruzi* [3], suggesting that some compounds are more prone than other to emerge as hits in any drug repositioning program, possibly due to their peculiar chemical structure, a possibility further discussed below when taking in consideration the "pan-assay interference compounds" (PAINS) issue.

The binding mode of the 11 repositioned drugs highlights how the DP1 occupied in F508del-CFTR by VX809 (here used as template) is a very large region that can be occupied more stably by very large molecules as antineoplastic agents that, making multiple interactions, display a lower complex energy and are consequently top-scored in the energy ranking (Table 1). Accordingly, the polycyclic natural compound rutin shows the lowest energy complex with F508del-CFTR thanks to its large dimension made up by the sugar moieties and a flavonic portion. Rutin is widely reported in literature as a very interesting molecule, endowed with diverse therapeutic effects, such as anti-cancer, anti-oxidant, adipogenesis suppressant and neuroprotective. However, *in vivo* rutin is rapidly converted in the flavonol quercetin by human gut bacteria [37,38], by removal of the disaccharide moiety, inferring the possibility that the beneficial effects of rutin may be actually mediated by quercetin. Relevant to this point, compared to rutin, quercetin and its derivatives are beneficial because of their more efficient absorption [43].

Our computational studies suggest that quercetin binds F508del-CFTR and that its binding region correspond to the DP1. Quercetin is a structural analogue of genistein. Interestingly, genistein is a F508del-CFTR potentiator previously demonstrated to bind almost the same region [44] that has been found to be shared by quercetin. This suggests the intriguing possibility that not only correctors, but also potentiators, are able to bind F508del-CFTR in the VX809 binding pocket, although the cryo-electron microscopy structure of potentiators ivacaftor and GLPG1837 with human CFTR showed that both compounds bind the same site within the transmembrane region [45].

In agreement with computational predictions, SPR analysis demonstrates that quercetin directly binds F508del-CFTR with an affinity that is comparable to that of VX809. More intriguingly, competition experiments indicated that while rutin competes with VX809 for the binding to F508del-CFTR, quercetin seems to succeed in interacting with F508del-CFTR along with VX809.

A possible interpretation of this behaviour is that quercetin act as a potentiator that binds to the flexible binding cleft spanning from NBD1 to ICL4 and NBD2 in such a way to produce a conformation of DP1 suitable for a better interaction of the corrector VX809.

Animal and human studies revealed that quercetin may alter the bioavailability of certain drugs [46], calling for further evaluation of its use in combination with drugs already administered to CF patients. Interestingly however, here we found that quercetin does not interfere with the binding of VX809 to F508del-CFTR. Accordingly, quercetin has been already reported to stimulate F508del-CFTR activity, in a dose-dependent manner, in FRT and CFBE41o- cells, kept at low temperature to allow rescue of the trafficking defect of mutant CFTR [40]. Interestingly, the observed increase in CFTR activity was not paralleled by an increase in intracellular cAMP levels [40]. In addition, nasal potential difference measurements performed in mice showed that perfusion with quercetin produced a hyperpolarization that was absent in $Cftr^{-/-}$ mice [40], further demonstrating that quercetin activates CFTR-mediated chloride secretion in airway epithelia *in vitro* and *in vivo*. Further investigation confirmed the ability of quercetin to induce CFTR-dependent hyperpolarization of the nasal potential difference and an increase of ciliary beat frequency when perfused in the nares of human, hypothesizing its use to promote mucociliary transport in individuals with rhinosinusitis [47].

Finally, quercetin was demonstrated to play a pleiotropic effect on chloride secretion, being able to stimulate also TMEM16A activity through different mechanisms which included elevation of Ca^{2+} concentration through L-type calcium channel and activation of basolateral NKCC, Na^+/K^+-ATPase, and K^+ channels [39].

Beside its actions of CFTR, quercetin has been found to act as a multitarget compound able to exert different activities, with its consequent inclusion among PAINS. This is a class of compounds with common substructural motifs that give them an increased chance of emerging as a hit in any assay or drug repositioning program [48]. The promiscuous effect of many of such compounds (including quercetin) is due to their capacity to act as aggregates [49] and are then usually considered less likely to be optimizable toward a useful compound. Appropriate electronic filters have been optimized to recognize PAINS in order to exclude them from further analysis, but more recently it has become increasingly clear their uncritical use may wrongly exclude useful compounds [50]. For what concern quercetin in particular, beside its direct action on CFTR described above, many of its other biological activities that identify it as PAINS make it also an interesting dietary supplement for CF patients:

I. It can be found in a variety of plants including citrus fruit and represents the larger part of our daily flavonoid intake. It could represent a valid food supplement for CF patients, exerting several positive effects due to its antioxidant activity. Acting as a free radical scavenger, quercetin may also be of help in reducing the chronic inflammation state which characterizes CF [51,52]. Accordingly, quercetin protects airways and lungs from lipopolysaccharide-induced acute lung injury [53,54].

II. Chronic pain in CF patients is well documented [55], being sometimes present as a side effect of CF therapies, as reported during use of fluoroquinolones and/or azole antifungal agents [56] and even Trikafta [17]. On the other hand, long term use of non-steroidal anti-inflammatory drugs raises concern due to their

renal toxicity, which may be increased in CF patients by the concomitant use of aminoglycosides. Relevant to pain treatment, quercetin is widely reported to exert a potent analgesic effect, intrinsically linked to its anti-inflammatory action [57,58], adding interest to a possible use of quercetin for CF patients.

III. It displays a good safety profile, having been granted approval as a food additive in Japan and being regarded as a safe antioxidant in the USA. Several studies on humans rarely reported adverse effects (however mild) following quercetin supplementation [46,59,60], while a number of literature studies suggest its beneficial use [61,62].

IV. Small molecules as quercetin could give a consistent contribution in the search of new CFTR modulators. Their smaller chemical structure, in comparison with antineoplastic agents or other natural compounds, makes them disadvantaged in the energy ranking, but their binding potential could be fruitfully investigated in fragment-based drug design approaches.

To date, CFTR drug design has been focused on the structure of VX809 and its analogues (e.g. VX445, VX661 and ARN23765). Differently, the superimposition of the drugs here repositioned opens new directions of investigation in some sub-regions between NBD1, NBD2 and ICL4, close to the VX809 binding-site (i.e. that occupied by a portion of imatinib, the one by rutin sugars and a third by a portion of the gliquidone scaffold) which represent interesting binding areas for the synthesis of tailored chemical structures. Interestingly, the aminoarylthiazole derivative EN503, endowed with a F508-del CFTR rescuing activity very similar to VX809 [24] showed to partially exploit two of these sub-regions in the alignment with imatinib, rutin and gliquidone. Thus, the very expanded family of aminoarylthiazole derivatives, that act as CFTR modulators, seems to be an additional operating space for the design and synthesis of new compounds.

In conclusion, in this work we designed a dedicated pipeline made up of bioinformatics and biochemical assays that allowed a pilot computational drug repositioning program applied to CF with the AIFA database. From the initial 846 drugs, 11 were repositioned onto F508del-CFTR. Of these, rutin was further investigated both for its favorable binding energy and for its interesting bioconversion to quercetin. This, beside proving the validity of our approach, allows to foresee that, enlarging the initial number of compounds to be screened, an equally higher number of hits will be identified.

4. Material and methods

4.1. Computational and analytical set-up

4.1.1. Drug-repositioning pipeline

A dedicated computational infrastructure was developed to accommodate all computational needs of the repositioning study (i.e. preparation of the dataset for repositioning, docking virtual screening and MDs). The pipeline was implemented on a High-Performance Computational Infrastructure base on OpenStack Hybrid Cloud Infrastructure including High Performance Storage, Multi Core Molecular Screening pipeline for docking studies and GPU based MDs.

Fig. 1 shows the pipeline that is composed of two main parts. The part A, already described in Ref. [24], processes an initial apo F508del-CFTR model embedded in DOPC lipid bilayer in order to find a set of MDs frames and the DP1 pocket of VX809. The Part B is the drug repositioning pipeline in which DP1 pocket from F508del-CFTR-VX809 complex [24] is firstly docked against AIFA library (see 4.1.2) with Autodock Vina (see 4.1.3). The resulting docking poses are filtered by binding energy, taking into account those with an energy like VX809, then by visual inspection, further considering the non-covalent interactions detected by PLIP [63], and by clinical and literature considerations. The remaining poses of relevant ligands are finally validated with MDs (Amber – see 4.1.3) by stability through RMSD and RMSF analysis. Moreover, a parallel path of the pipeline processes the F508del-CFTR apo form frames from the previous study [24] by means of Fpocket (see 4.1.4) to find all druggable pockets along the dynamics and to compare them with the key residues surrounding the ligand selected poses.

4.1.2. Preparation of the dataset for repositioning

The database used for the present study was obtained starting from the approved list of the AIFA drugs containing 1130 compounds [<u>www.farmaci.agenziafarmaco.gov.it/bancadati-farmaci</u>], excluding not appropriate molecules (such as inorganic salts, peptides, proteins and hormones, contrast agents) thus obtaining a set of 846 small-molecule drugs. When the molecule showed chiral centres, all available configurations were considered. 3D structures of drugs were downloaded from the Zinc database [64]. The F508del-CFTR protein model already reported [24] was used for the repositioning task. The choice has been done taking into account that it displays good stereo-chemical parameters, favorable agreement with experimental data [36] and with the available human cryo E.M. models and potential physiological relevance, since it refers to a chloride channel protein in its close state.

4.1.3. Docking and MDs

Docking and MDs simulations were performed following computational protocol already defined [24]. The docking software (Autodock Vina) has been used with the exhaustiveness parameter of 24, and the other parameters as default. The drug repositioning was based on the frames from the MDs of the apo F508del-CFTR and of F508del-CFTR-VX809 complex, already selected in the same study cited above. The grid boxes were centred on the geometric centre of DP1. Three independent MDs (AMBER-14 package) analyses for each complex were carried out using ff12SB force field for the protein, phosaa10 for the modified residues of the protein, and lipid14 for the DOPC lipid bilayer. The complexes were solvated with TIP3P water model and neutralized by the addiction of counter ions. The following parameterization for the simulations was used: (1) Twelve minimizations of 5000 steps with decreasing restraints on the whole system, and a thirteenth minimization of 50000 steps without restraints, checking the reaching of the system energy plateau. The non-bonded cut-off was set at 8 Å. (2) Heating NVT, increasing temperature (T) from 0 K to 100 K in 50 ps, then 50 ps at constant 100 K with 6 kcal/mol restraint for either protein and ligand; then 75 ps increasing T from 100 K to 300 K and 25 ps at constant 300 K with 4 kcal/mol and 6 kcal/mol restraint for protein and ligand, respectively, checking the reaching of the desired temperature. (3) Equilibration NPT of 4 ns at constant 300 K with a restraint of 2 kcal/mol and 6 kcal/mol for protein and ligand, respectively. From equilibration, each independent simulation was carried out using different initial velocities. (4) MDs production of 25 ns without any restraints.

The clusterization of the initial apo model has been performed with AmberTools (cpptraj).

4.1.4. MM-GBSA analyses

The Molecular Mechanics Generalized Born Surface Area (MM-GBSA) analysis was performed for each simulation using AmberTools (MMPBSA.py) to obtain the binding free energy (ΔG) between the ligand (rutin, telmisartan or tadalafil) and the receptor (F508del-CFTR). To perform the analysis, snapshots were obtained from the last 400 ps of each simulation, setting igb = 5 and the ionic strength to 0.100.

4.1.5. Fpocket analysis

Fpocket analysis has been performed outside the pipeline with the default parameters in order to evaluate the druggability of the selected pockets. The program Fpocket allows the identification of druggable cavities on protein complexes from multiple structures sampled in MDs frames and gives for each pocket a druggability score, which we used to analyze the obtained results. Fpocket has been used to compute the best druggable pockets along the trajectory of the MDs (1250 frames spaced by 20 ps). For each frame the number of residues of the pocket that belong to a predetermined set (in particular imatinib and VX809 sub pockets) has been computed and plotted to evaluate a sort of druggability score of these pocket residues along the dynamics.

4.2. Reagents

His-tagged human intact F508del-CFTR protein purified as described [65,66] was provided by Prof. R.C. Ford, Manchester University, UK. Lipids [synthetic phospholipid blend (Dioleoyl) DOPC:DOPS (7:3 w/w)] from Avanti Polar Lipids, Alabaster, AL. CHAPS and cholesteryl hemisuccinate (CHS) Tris salt from Sigma-Aldrich, St Louis, MO. Carboxy-methyl dextran CM5 sensorchip, anti-His antibody, 1-ethyl-3-(3-diaminopropyl)-carbodiimide hydro-chloride and N-hydroxysuccinimide (NHS) from GE-Healthcare, Milwaukee, WI. VX809 was from Selleck Chemicals, Houston TX. Rutin, Tadalafil and Telmisartan were from TargetMol, Wellesley Hills, MA. Quercetin was from Merck Life Science s.r.l. Milan, Italy.

4.3. Surface plasmon resonance

A BIAcore X-100 instrument (GE-Healthcare) was used. The biosensor containing F508del-CFTR in a membrane-like lipid environment was prepared as described [24]. Briefly, anti-His antibody was immobilized on a CM5 sensorchip by standard amine-coupling chemistry. After sensorchip equilibration by injection of DOPC:DOPS (7:3 W/W) 0.075 μg/ml, 0.02% CHS, 0.1% CHAPS (DOPC:DOPS running buffer)), human His-tagged intact F508del-CFTR (10 μg/ml, Hepes 50 mM, pH 7 containing NaCl 150 mM DOPC: DOPS (7:3 W/W) 363 μg/ml, 0.06% CHS, 0.3% CHAPS (DOPC:DOPS-F508del-CFTR buffer), was injected on the anti-His surface, allowing the capture of about 41 RU. A sensorchip coated with anti-His antibody alone was used for blank subtraction.

To evaluate their F508del-CFTR-binding capacity, compounds were injected over the sensorchip at increasing concentration in PBS, 0.05% surfactant P20 and 5% DMSO, pH 7.4 (PBS-DMSO) by adopting the single cycle model [67]. Dissociation Constant (Kd) values were calculated by steady state analyses performed by fitting the proper form of Scatchard's equation for the plot of the bound resonance units (RU) at equilibrium *versus* the compound concentration in solution by means of the BIAEVALUATION software embedded in the BIAcore X-100 instrument. VX809 was used as positive control.

For competition assays, VX809 (75 μM) was injected alone or in the presence of rutin or of quercetin (both at 150 μM) onto the F508del-CFTR-biosensor. RU values were then measured at equilibrium.

Notes

The authors declare no competing financial interest.

Credit author contribution statement

AO: funding acquisition, software development, data curation. MU: docking repositioning and MDs calculations, review & editing. MR: funding acquisition, supervision, writing, review & editing, project administration. CU: methodology, investigation (SPR analysis). NP: analysis and interpretation of biological data. EP: biological evaluation of compounds activity as CFTR modulators. MM: software development. RP: clinical consulting. EC: review & editing. PF: funding acquisition, conceptualization, computational data analysis, writing, review & editing. PD: pipeline design, conceptualization, computational data analysis, writing, review & editing.

Declaration of competing interest

The authors declare that they have no known competing financial interests or personal relationships that could have appeared to influence the work reported in this paper.

Acknowledgments

We wish to thank Prof. Robert C. Ford, University of Manchester, UK for providing purified intact human F508del-CFTR protein and Dr. G. Righetti and Dr. L. Khabibulina for their support to calculations.

Appendix A. Supplementary data

Supplementary data to this article can be found online at https://doi.org/10.1016/j.ejmech.2021.113186.

Funding

This research was funded by Fondazione Italiana Fibrosi Cistica, project FFC #10/2019 to MR, PF and AO (Delegation of Vittoria Ragusa, Siracusa e Catania Mascalucia) and FFC #9/2019 to NP (Delegazione FFC di Genova con Gruppo di sostegno FFC di Savona Spotorno, Delegazione FFC di Valle Scrivia Alessandria, Delegazione FFC di Montescaglioso, Delegazione FFC di Ascoli Piceno).

Italian Ministry of Education, University and Research (MIUR) PON ELIXIR (PIR01_00017) and CNRbiOmics, from pan-European research infrastructure for Biobanking and BioMolecular Resources Research Infrastructure (BBMRI) for AO and PD. Work in NP lab is also supported by the Italian Ministry of Health through Cinque per Mille and Ricerca Corrente (Linea 1).

References

[1] T. Pillaiyar, S. Meenakshisundaram, M. Manickam, M. Sankaranarayanan, A medicinal chemistry perspective of drug repositioning: recent advances and challenges in drug discovery, Eur. J. Med. Chem. 195 (2020) 112275.
[2] K. Park, A review of computational drug repurposing, Transl Clin Pharmacol 27 (2019) 59–63.
[3] E.E. Lara-Ramirez, J.C. Lopez-Cedillo, B. Nogueda-Torres, M. Kashif, C. Garcia-Perez, V. Bocanegra-Garcia, R. Agusti, M.L. Uhrig, G. Rivera, An in vitro and in vivo evaluation of new potential trans-sialidase inhibitors of Trypanosoma cruzi predicted by a computational drug repositioning method, Eur. J. Med. Chem. 132 (2017) 249–261.
[4] R. Rivas Caldas, S. Boisrame, Upper aero-digestive contamination by Pseudomonas aeruginosa and implications in Cystic Fibrosis, J. Cyst. Fibros. 14 (2015) 6–15.

[5] T.S. Scott-Ward, M.D. Amaral, Deletion of Phe508 in the first nucleotide-binding domain of the cystic fibrosis transmembrane conductance regulator increases its affinity for the heat shock cognate 70 chaperone, FEBS J. 276 (2009) 7097–7109.
[6] M.D. Amaral, C.M. Farinha, Rescuing mutant CFTR: a multi-task approach to a better outcome in treating cystic fibrosis, Curr. Pharmaceut. Des. 19 (2013) 3497–3508.
[7] M.P. Rogan, D.A. Stoltz, D.B. Hornick, Cystic fibrosis transmembrane conductance regulator intracellular processing, trafficking, and opportunities for mutation-specific treatment, Chest 139 (2011) 1480–1490.
[8] P. Fanen, A. Wohlhuter-Haddad, A. Hinzpeter, Genetics of cystic fibrosis: CFTR mutation classifications toward genotype-based CF therapies, Int. J. Biochem. Cell Biol. 52 (2014) 94–102.
[9] J.S. Elborn, Cystic fibrosis, Lancet 388 (2016) 2519–2531.
[10] A.R. Habib, M. Kajbafzadeh, S. Desai, C.L. Yang, K. Skolnik, B.S. Quon, A systematic review of the clinical efficacy and safety of CFTR modulators in cystic fibrosis, Sci. Rep. 9 (2019) 7234.
[11] C.E. Bear, A therapy for most with cystic fibrosis, Cell 180 (2020) 211.
[12] G. Veit, A. Roldan, M.A. Hancock, D.F. Da Fonte, H. Xu, M. Hussein, S. Frenkiel, E. Matouk, T. Velkov, G.L. Lukacs, Allosteric folding correction of F508del and rare CFTR mutants by elexacaftor-tezacaftor-ivacaftor (Trikafta) combination, JCI Insight 5 (2020).
[13] M. Higgins, N. Volkova, K. Moy, B.C. Marshall, D. Bilton, Real-World outcomes among patients with cystic fibrosis treated with ivacaftor: 2012-2016 experience, Pulm Ther 6 (2020) 141–149.
[14] N. Volkova, K. Moy, J. Evans, D. Campbell, S. Tian, C. Simard, M. Higgins, M.W. Konstan, G.S. Sawicki, A. Elbert, S.C. Charman, B.C. Marshall, D. Bilton, Disease progression in patients with cystic fibrosis treated with ivacaftor: data from national US and UK registries, J. Cyst. Fibros. 19 (2020) 68–79.
[15] H.G.M. Heijerman, E.F. McKone, D.G. Downey, E. Van Braeckel, S.M. Rowe, E. Tullis, M.A. Mall, J.J. Welter, B.W. Ramsey, C.M. McKee, G. Marigowda, S.M. Moskowitz, D. Waltz, P.R. Sosnay, C. Simard, N. Ahluwalia, F. Xuan, Y. Zhang, J.L. Taylor-Cousar, K.S. McCoy, Efficacy and safety of the elexacaftor plus tezacaftor plus ivacaftor combination regimen in people with cystic fibrosis homozygous for the F508del mutation: a double-blind, randomised, phase 3 trial, Lancet 394 (2019) 1940–1948.
[16] W. Tindell, A. Su, S.M. Oros, A.O. Rayapati, G. Rakesh, Trikafta and Psychopathology in Cystic Fibrosis: A Case Report, Psychosomatics, 2020.
[17] S.M. Rotolo, S. Duehlmeyer, S.M. Slack, H.R. Jacobs, B. Heckman, Testicular pain following initiation of elexacaftor/tezacaftor/ivacaftor in males with cystic fibrosis, J. Cyst. Fibros. 19 (2020) e39–e41.
[18] A. Gramegna, M. Contarini, S. Aliberti, R. Casciaro, F. Blasi, C. Castellani, From ivacaftor to triple combination: a systematic review of efficacy and safety of CFTR modulators in people with cystic fibrosis, Int. J. Mol. Sci. 21 (2020).
[19] L. da Silva Filho, M. Zampoli, M. Cohen-Cymberknoh, S.K. Kabra, Cystic fibrosis in low and middle-income countries (LMIC): a view from four different regions of the world, Paediatr. Respir. Rev. (2020), https://doi.org/10.1016/j.prrv.2020.07.004. S1526-0542(20)30108-1.
[20] S.P. Newman, Delivering drugs to the lungs: the history of repurposing in the treatment of respiratory diseases, Adv. Drug Deliv. Rev. 133 (2018) 5–18.
[21] S.D. Anderson, E. Daviskas, J.D. Brannan, H.K. Chan, Repurposing excipients as active inhalation agents: the mannitol story, Adv. Drug Deliv. Rev. 133 (2018) 45–56.
[22] V.R. Villella, A. Tosco, S. Esposito, G. Bona, V. Raia, L. Maiuri, Mutation-specific therapies and drug repositioning in cystic fibrosis, Minerva Pediatr. 71 (2019) 287–296.
[23] B.Z. Schmidt, J.B. Haaf, T. Leal, S. Noel, Cystic fibrosis transmembrane conductance regulator modulators in cystic fibrosis: current perspectives, Clin. Pharmacol. 8 (2016) 127–140.
[24] P. D'Ursi, M. Uggeri, C. Urbinati, E. Millo, G. Paiardi, L. Milanesi, R.C. Ford, J. Clews, X. Meng, P. Bergese, A. Ridolfi, N. Pedemonte, P. Fossa, A. Orro, M. Rusnati, Exploitation of a novel biosensor based on the full-length human F508de1-CFTR with computational studies, biochemical and biological assays for the characterization of a new Lumacaftor/Tezacaftor analogue, Sensor. Actuator. B Chem. 301 (2019).
[25] V. Le Guilloux, P. Schmidtke, P. Tuffery, Fpocket: an open source platform for ligand pocket detection, BMC Bioinf. 10 (2009) 168.
[26] V.M. Sofia, C. Surace, V. Terlizzi, L. Da Sacco, F. Alghisi, A. Angiolillo, C. Braggion, N. Cirilli, C. Colombo, A. Di Lullo, R. Padoan, S. Quattrucci, V. Raia, G. Tuccio, F. Zarrilli, A.C. Tomaiuolo, A. Novelli, V. Lucidi, M. Lucarelli, G. Castaldo, A. Angioni, Trans-heterozygosity for mutations enhances the risk of recurrent/chronic pancreatitis in patients with Cystic Fibrosis, Mol Med 24 (2018) 38.
[27] S.P. Conway, C. Etherington, D.G. Peckham, A. Whitehead, A pilot study of zafirlukast as an anti-inflammatory agent in the treatment of adults with cystic fibrosis, J. Cyst. Fibros. 2 (2003) 25–28.
[28] D. O'Shea, J. O'Connell, Cystic fibrosis related diabetes, Curr. Diabetes Rep. 14 (2014) 511.
[29] Y. Wang, S. Qiao, D.W. Han, X.R. Rong, Y.X. Wang, J.J. Xue, J. Yang, Telmisartan improves insulin resistance: a meta-analysis, Am. J. Therapeut. 25 (2018) e642–e651.
[30] C. Colombo, M.C. Russo, L. Zazzeron, G. Romano, Liver disease in cystic fibrosis, J. Pediatr. Gastroenterol. Nutr. 43 (Suppl 1) (2006) S49–S55.
[31] B. Lubamba, J. Lebacq, G. Reychler, E. Marbaix, P. Wallemacq, P. Lebecque, T. Leal, Inhaled phosphodiesterase type 5 inhibitors restore chloride transport in cystic fibrosis mice, Eur. Respir. J. 37 (2011) 72–78.
[32] A. Schultz, S. Stick, Early pulmonary inflammation and lung damage in children with cystic fibrosis, Respirology 20 (2015) 569–578.
[33] K. Liu, H. Kokubo, Exploring the stability of ligand binding modes to proteins by molecular dynamics simulations: a cross-docking study, J. Chem. Inf. Model. 57 (2017) 2514–2522.
[34] K. Liu, E. Watanabe, H. Kokubo, Exploring the stability of ligand binding modes to proteins by molecular dynamics simulations, J. Comput. Aided Mol. Des. 31 (2017) 201–211.
[35] K. Liu, H. Kokubo, Prediction of ligand binding mode among multiple cross-docking poses by molecular dynamics simulations, J. Comput. Aided Mol. Des. 34 (2020) 1195–1205.
[36] M. Rusnati, P. D'Ursi, N. Pedemonte, C. Urbinati, R.C. Ford, E. Cichero, M. Uggeri, A. Orro, P. Fossa, Recent strategic advances in CFTR drug discovery: an overview, Int. J. Mol. Sci. 21 (2020).
[37] A. Amaretti, S. Raimondi, A. Leonardi, A. Quartieri, M. Rossi, Hydrolysis of the rutinose-conjugates flavonoids rutin and hesperidin by the gut microbiota and bifidobacteria, Nutrients 7 (2015) 2788–2800.
[38] N.R. Shin, J.S. Moon, S.Y. Shin, L. Li, Y.B. Lee, T.J. Kim, N.S. Han, Isolation and characterization of human intestinal Enterococcus avium EFEL009 converting rutin to quercetin, Lett. Appl. Microbiol. 62 (2016) 68–74.
[39] B. Yu, Y. Jiang, L. Jin, T. Ma, H. Yang, Role of quercetin in modulating chloride transport in the intestine, Front. Physiol. 7 (2016) 549.
[40] L.C. Pyle, J.C. Fulton, P.A. Sloane, K. Backer, M. Mazur, J. Prasain, S. Barnes, J.P. Clancy, S.M. Rowe, Activation of the cystic fibrosis transmembrane conductance regulator by the flavonoid quercetin: potential use as a biomarker of DeltaF508 cystic fibrosis transmembrane conductance regulator rescue, Am. J. Respir. Cell Mol. Biol. 43 (2010) 607–616.
[41] R. Maitra, J.W. Hamilton, Altered biogenesis of deltaF508-CFTR following treatment with doxorubicin, Cell. Physiol. Biochem. 20 (2007) 465–472.
[42] H. Joensuu, Treatment of inoperable gastrointestinal stromal tumor (GIST) with Imatinib (Glivec, Gleevec), Med. Klin. 97 (2002) 28–30.
[43] T. Makino, R. Shimizu, M. Kanemaru, Y. Suzuki, M. Moriwaki, H. Mizukami, Enzymatically modified isoquercitrin, alpha-oligoglucosyl quercetin 3-O-glucoside, is absorbed more easily than other quercetin glycosides or aglycone after oral administration in rats, Biol. Pharm. Bull. 32 (2009) 2034–2040.
[44] O. Moran, L.J. Galietta, O. Zegarra-Moran, Binding site of activators of the cystic fibrosis transmembrane conductance regulator in the nucleotide binding domains, Cell. Mol. Life Sci. 62 (2005) 446–460.
[45] F. Liu, Z. Zhang, A. Levit, J. Levring, K.K. Touhara, B.K. Shoichet, J. Chen, Structural identification of a hotspot on CFTR for potentiation, Science 364 (6446) (2019) 1184–1188.
[46] S. Andres, S. Pevny, R. Ziegenhagen, N. Bakhiya, B. Schafer, K.I. Hirsch-Ernst, A. Lampen, Safety aspects of the use of quercetin as a dietary supplement, Mol. Nutr. Food Res. 62 (2018).
[47] S. Zhang, N. Smith, D. Schuster, C. Azbell, E.J. Sorscher, S.M. Rowe, B.A. Woodworth, Quercetin increases cystic fibrosis transmembrane conductance regulator-mediated chloride transport and ciliary beat frequency: therapeutic implications for chronic rhinosinusitis, Am J Rhinol Allergy 25 (2011) 307–312.
[48] J.B. Baell, Feeling nature's PAINS: natural Products, natural product drugs, and Pan assay interference compounds (PAINS), J. Nat. Prod. 79 (2016) 616–628.
[49] S.L. McGovern, B.K. Shoichet, Kinase inhibitors: not just for kinases anymore, J. Med. Chem. 46 (2003) 1478–1483.
[50] J.B. Baell, J.W.M. Nissink, Seven year itch: pan-assay interference compounds (PAINS) in 2017-utility and limitations, ACS Chem. Biol. 13 (2018) 36–44.
[51] Y.S. Yi, Regulatory roles of flavonoids on inflammasome activation during inflammatory responses, Mol. Nutr. Food Res. 62 (2018), e1800147.
[52] K.B.R. Belchamber, L.E. Donnelly, Targeting defective pulmonary innate immunity - a new therapeutic option? Pharmacol. Ther. (2020) 107500.
[53] C.H. Yeh, J.J. Yang, M.L. Yang, Y.C. Li, Y.H. Kuan, Rutin decreases lipopolysaccharide-induced acute lung injury via inhibition of oxidative stress and the MAPK-NF-kappaB pathway, Free Radic. Biol. Med. 69 (2014) 249–257.
[54] S.C. Shen, W.R. Lee, H.Y. Lin, H.C. Huang, C.H. Ko, L.L. Yang, Y.C. Chen, In vitro and in vivo inhibitory activities of rutin, wogonin, and quercetin on lipopolysaccharide-induced nitric oxide and prostaglandin E(2) production, Eur. J. Pharmacol. 446 (2002) 187–194.
[55] E.A. Clarke, P. Watson, J.E. Freeston, D.G. Peckham, A.M. Jones, A. Horsley, Assessing arthritis in the context of cystic fibrosis, Pediatr. Pulmonol. 54 (2019) 770–777.
[56] L.L. Benitez, P.L. Carver, Adverse effects associated with long-term administration of azole antifungal agents, Drugs 79 (2019) 833–853.
[57] G. Carullo, A.R. Cappello, L. Frattaruolo, M. Badolato, B. Armentano, F. Aiello, Quercetin and derivatives: useful tools in inflammation and pain management, Future Med. Chem. 9 (2017) 79–93.
[58] A.K. Singh, S. Kumar, M. Vinayak, Recent development in antihyperalgesic effect of phytochemicals: anti-inflammatory and neuro-modulatory actions, Inflamm. Res. 67 (2018) 633–654.
[59] T. Okamoto, Safety of quercetin for clinical application (Review), Int. J. Mol. Med. 16 (2005) 275–278.
[60] N.T. Lu, C.M. Crespi, N.M. Liu, J.Q. Vu, Y. Ahmadieh, S. Wu, S. Lin, A. McClune, F. Durazo, S. Saab, S. Han, D.C. Neiman, S. Beaven, S.W. French, A phase I dose escalation study demonstrates quercetin safety and explores potential for bioflavonoid antivirals in patients with chronic hepatitis C, Phytother Res. 30 (2016) 160–168.

[61] M.K. Han, T.A. Barreto, F.J. Martinez, A.T. Comstock, U.S. Sajjan, Randomised clinical trial to determine the safety of quercetin supplementation in patients with chronic obstructive pulmonary disease, BMJ Open Respir Res 7 (2020), e000392.
[62] K.B.R. Belchamber, L.E. Donnelly, Targeting defective pulmonary innate immunity - a new therapeutic option? Pharmacol. Ther. 209 (2020) 107500.
[63] S. Salentin, S. Schreiber, V.J. Haupt, M.F. Adasme, M. Schroeder, PLIP: fully automated protein-ligand interaction profiler, Nucleic Acids Res. 43 (W1) (2015) W443–W447.
[64] T. Sterling, J.J. Irwin, ZINC 15–ligand discovery for everyone, J. Chem. Inf. Model. 55 (2015) 2324–2337.
[65] L. O'Ryan, T. Rimington, N. Cant, R.C. Ford, Expression and purification of the cystic fibrosis transmembrane conductance regulator protein in Saccharomyces cerevisiae, JoVE (2012), https://doi.org/10.3791/3860.
[66] N. Pollock, N. Cant, T. Rimington, R.C. Ford, Purification of the cystic fibrosis transmembrane conductance regulator protein expressed in Saccharomyces cerevisiae, JoVE (2014), https://doi.org/10.3791/51447.
[67] H.H. Trutnau, New multi-step kinetics using common affinity biosensors saves time and sample at full access to kinetics and concentration, J. Biotechnol. 124 (2006) 191–195.